

# A PROBABILISTIC MECHANICS APPROACH TO DIE CRACKING PREDICTION IN FLIP-CHIP BALL GRID ARRAY PACKAGE

Jie-Hua Zhao

Motorola, Semiconductor Products Sector, MD:TX30/OE21

6501 William Cannon Drive West, Austin, TX 78735

Tel: 512-895-7353, Fax: 512-895-7149

Email: Jie-Hua.Zhao@motorola.com

## ABSTRACT

Flip-chip plastic ball grid array (FC-PBGA) packages are widely used in high performance components. However, its die back is normally under tensile stress at low temperatures. This paper presents a probabilistic mechanics approach to predict the die failure rate in the FC-PBGA qualification process. The methodology consists of three parts: i) die strength test using four-point bending (4PB) method; ii) the radius of curvature (ROC) measurement of the assembled FC-PBGA at room temperature; iii) Finite element method (FEM) stress analysis. In the first part, a specially modified 3-parameter Weibull function is used to fit the 4PB die strength data. The three parameters of the Weibull distribution are used as the sole description of the cracking characteristics for a specific die process in the late analysis. In the second part, the measured ROC of FC-PBGA at room temperature is used as a calibration input to determine the effective stress-free temperature of the FC-PBGA. It is used to overcome the difficulty caused by process-induced residual stress and unknown material properties, e.g., viscoelasticity the underfill and plastic substrate that are normally unavailable. This effective stress-free temperature can be used in the stress analysis in the third part of the mentioned methodology. In the third part, FEM is used to calculate the die stress distribution under most critical stage of certain qualification process. The calculated stress distribution is combined with the Weibull distribution parameters of die strength test to predict the die failure percentage.

**KEY WORDS:** Die cracking, Weibull, 4-point bend, probabilistic mechanics, finite element method.

## NOMENCLATURE

<b>4PB:</b>	four point bending
<b>FC:</b>	flip-chip
<b>FC-PBGA:</b>	flip chip plastic ball grid array
<b>C4:</b>	Controlled Collapse Chip Connection, also referred as solder bumps
<b>C5:</b>	Controlled Collapse Chip Carrier Connection, also referred as solder balls or spheres
<b>CTE:</b>	coefficient of thermal expansion
<b>FEM:</b>	finite element method
<b>CDF:</b>	cumulative distribution function
<b>ANSYS:</b>	a general purpose finite element method software which is commercially available

## INTRODUCTION

Flip-chip packages have excellent electric performance and high I/O density. Flip-chip plastic ball grid array (FC-PBGA) packages have better board level solder joint reliability, better electric performance and lower cost than their ceramic counterpart flip-chip ceramic ball grid array packages. However, in FC-PBGA packages, silicon die is attached on a plastic laminate substrate by solder bump joints. Underfill material is usually filled in the gap between the die and the substrate to protect the solder joints for better reliability. After the underfilling process, the die and substrate are rigidly bonded and no interface delaminations and separations should be present. A silicon die, with a coefficient of thermal expansion (CTE) of 2.6 ppm/°C, and a plastic laminate substrate, with a CTE from 15 to 25 ppm/°C, are rigidly bonded by a thin layer of underfill material. As a result of the CTE mismatch, significant thermal stress occurs in the die and the substrate during thermal cycling. In the component level reliability test, this thermal stress is the major cause of many failure modes including die cracking.

In order to avoid die cracking, there are several measures can be taken. One is to reduce the tensile stress on the back of the die by proper package design. For example, a metal lid can be added on top of the die back using a layer of adhesive [1]. This may reduce the bending of die and even put the die in compressive stress, which reduces die cracking risk. Adding a lid to the FC-PBGA, adds cost to the device and also introduces two more interfaces which may add delamination risk. Moreover, cost reduction consideration is always a major driving force for other remedies. In fact, process-related improvements are also effective to achieve a lower die stress, such as grinding the die to change the thickness ratio of die and substrate [2]. The other aspect of avoiding die cracking from process related aspect is to maintain the silicon die at a high strength. The theoretical strength of the die is about the order of the silicon shear modulus [3] [4], which is in the order of 100,000 MPa. The actual strength of the die falls down to hundreds of MPa. This is commonly attributed to the existence of surface flaws. Surface flaws create stress concentrations near the die surface when it is under tension. The difference of the die strength between ideal value and the actual values suggests that there is a lot of room for process control to increase actual die strength.

Silicon is normally brittle at the temperature interested. The stress at the stress concentration points caused by defects can easily exceed the theoretical strength and therefore break the

die while the nominal stress is around a couple of hundreds of MPa. Surface scratches and edge chipping is sometimes inevitable for specific processes and therefore die cracking is one of the major concerns in flip-chip package development.

To evaluate a certain process of die preparation and ensure that it is proper for flip-chip package, the die strength measurement is required. The die strength testing is usually conducted on bending test, such as the 4-point bending (4PB) test [5]. A recent work provides a methodology of failure prediction using the 4PB-tested die strength and the finite element method (FEM)-calculated die stress distribution [6]. This paper is going to use the aforementioned methodology on FC-PBGA and study how the dicing process control affects the die cracking risk.

### THEORY

As discussed in Reference [6], following the essence Weibull presented in his hallmark paper [7], we propose the following Weibull cumulative density function (CDF) for die strength measurement data:

$$P_f = 1 - \exp \left[ -\Gamma \left( \frac{1}{m} + 1 \right) \left( \frac{\sigma_{nom} - \sigma_0}{\sigma_f} \right)^m \frac{A}{a} S(A) \right] \quad (1)$$

with a stress area integral

$$S(A) = \frac{1}{A} \int_A \left( \frac{(\sigma_1 - \sigma_0)H(\sigma_1 - \sigma_0)}{\sigma_{nom} - \sigma_0} \right)^m + \left( \frac{(\sigma_2 - \sigma_0)H(\sigma_2 - \sigma_0)}{\sigma_{nom} - \sigma_0} \right)^m + \left( \frac{(\sigma_3 - \sigma_0)H(\sigma_3 - \sigma_0)}{\sigma_{nom} - \sigma_0} \right)^m dA \quad (2)$$

Where  $\sigma_0$  is the cut-off stress which needs to be determined by the data fitting;  $\sigma_f$  is the unit area strength of the die;  $\sigma_{nom}$  is the nominal strength of the die, usually the measured maximum stress at which the die fails;  $P_f$  is the failure probability of the die;  $m$  is the Weibull modulus;  $A$  is the die surface area under tension;  $a$  is the unit surface area (1 mm<sup>2</sup> is chosen here);  $\sigma_1$ ,  $\sigma_2$ , and  $\sigma_3$  are three principal stresses;  $\Gamma$  is the gamma function; and  $H(\sigma)$  is the step function, which is defined to account for the fact that compressive stress normally does not contribute to die cracking:

$$H(\sigma) = \begin{cases} 1, & \text{if } \sigma > 0 \\ 0, & \text{if } \sigma < 0 \end{cases} \quad (3)$$

The three parameters  $\sigma_f$ ,  $\sigma_0$  and  $m$  are unknown and need to be determined from the experimental data by data-fitting.

The basic assumptions we have made in Equation (1) are the following: (i) The material is isotropic and statistically homogenous which means the probability of finding a flaw with a given severity in a given surface is uniform throughout the surface of the die. (ii) Once the crack has initiate, it will propagate without further increase in load, resulting in fracture. (iii) The contribution a flaw makes to the failure probability of a loaded die is independent of the position of the flaw on the die surface. (iv) The three principal stresses acting at a general point contribute independently to the failure probability [6] [8].

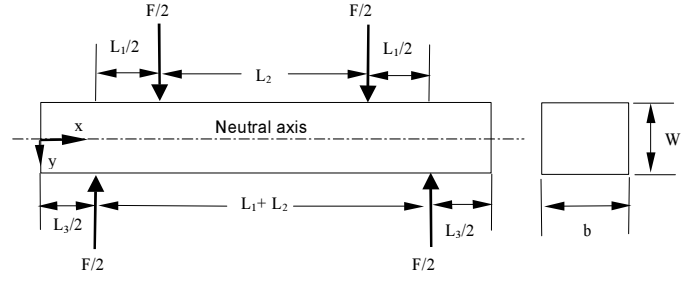


Fig. 1. Schematic of 4-point bend die strength test.

The real advantage of using Equations (1) and (2), is that they can relate the tested die strength to die failure rate for die under complicated loading in packages. This includes the following aspects: 1) the die top in the 4PB test is under uniaxial tensile stress and the die in FC-PBGA is under multi-axial stress; 2) the 4PB only puts part of the die top under tension and the die top in FC-PBGA package has almost 100% of its area under tension in most situations; 3) the die stress at its side edges and the portions of the 4PB between the inner span and outside span (i.e., the  $L_1/2$  portions shown in Figure 1) also have contribution to the die fracturing probability during test.

From 4-point bending test data, we can determine the three parameters  $\sigma_f$ ,  $\sigma_0$  and  $m$ . These three parameters are assumed to be independent of the stress state and sample geometry. Finite element method is often used to calculate the die stress in FC-PBGA. The distribution of the three principal stresses  $\sigma_1$ ,  $\sigma_2$  and  $\sigma_3$  can be calculated by FEM. Let's assume, for example,  $\sigma_{nom} = \text{Max}(\sigma_1)$  and use Equation (2) to calculate the stress-area integral  $S(A)$  for the die in a specific package. Then, the die failure rate can be easily obtained from Equation (1). In the above procedure, we have used an essential postulation, which is that these three fitting parameters ( $\sigma_f$ ,  $\sigma_0$  and  $m$ ) can fully characterize the die breaking process both in the 4-point bending test and in the flip-chip assembly and testing application. Therefore, it is fair to say that these three parameters are equivalent to a set of material property parameters to describe the die fracture process in terms of probabilistic mechanics. The contribution of the stress distribution and sample geometry are taken care of by the stress-area integral Equation (2). The probabilistic mechanics methodology we are presenting here has separated the material aspect from the loading and geometry aspect of the system. The material aspect is solely characterized by the three fitting parameters of the Weibull function. The loading and geometry aspect is taken into account by the stress-area integral.

The stress-area integral Equation (2) seems complicated. It actually can be evaluated analytically in the 4-point bend configuration and reduced to an explicit closed-form expression. In complicated stress states, such as in the FC-PBGA package case, a numerical integration must be employed to calculate the stress-area integral.

A schematic of the 4-point bending experiment is shown in

Figure 1. The die is under pure bending. The stress at the inner loading span is uniform. The material strength theory gives the following simple relation [9],

$$\sigma = \frac{3FL_1}{2bW^2} \quad (4)$$

The strength of the die is calculated by Equation (4) when the load is at the breaking point. The stress calculated by Equation (4) is called the nominal stress  $\sigma_{nom}$ . The detailed tensile stress distribution in a sample die under 4-point bending load is [10]:

$$\sigma(x, y, z) = \begin{cases} \sigma_{nom} & \text{(die bottom surface in the inner span)} \\ \frac{2x\sigma_{nom}}{L_1} & \text{(die bottom between inner and outer spans)} \\ \frac{2y\sigma_{nom}}{W} & \text{(die side within inner span)} \\ \frac{4xy\sigma_{nom}}{L_1W} & \text{(die side between inner and outer spans)} \end{cases} \quad (5)$$

The principal stress components for the 4-point bending configuration are simple. Only one component is non-vanishing and the other two components are zero. Therefore, Equation (5) is simply the principal stress expression, which is  $\sigma_1$ . Plugging Equation (5) in Equation (2), the stress-area integral can be evaluated. Since the thickness of the die is usually thin and the stress on the die side surfaces between the inner and outer spans is less than nominal stress, the contribution of the fourth line in Equation (5) can be neglected for simplicity purpose. Therefore, the evaluated stress-area integral for 4PB test is

$$S(A) = \frac{1}{(L_1 + L_2)(b + W)} \times \left[ \frac{L_2W + bL_1}{1 + m} \left( 1 - \frac{\sigma_0}{\sigma_{nom}} \right) + bL_2 \right] \quad (6)$$

It should be point out that in the evaluation of the stress-area integral, the area  $A$  is that under tensile stress. In order to be consistent with Equation (2),  $A$  in Equation (1) should be also the area under tension, which is  $A = (W + b)(L_1 + L_2)$ . Recall that we have assumed the unit area  $a = 1\text{mm}^2$ , Equation (1) becomes

$$P_f = 1 - \exp \left[ -\Gamma \left( \frac{1}{m} + 1 \right)^m \left( \frac{\sigma_{nom} - \sigma_0}{\sigma_f} \right)^m \right] \times \left[ \frac{L_2W + bL_1}{1 + m} \left( 1 - \frac{\sigma_0}{\sigma_{nom}} \right) + bL_2 \right] \quad (7)$$

In Equation (7), the three parameters  $\sigma_f$ ,  $\sigma_0$  and  $m$  are unknown and need to be determined by the data-fitting procedure. The 4-point bending die strength measurement can provide data points of  $\sigma_{nom}$  and  $P_f$ . The parameters  $L_1$ ,  $L_2$  and  $W$  are defined by the experimental apparatus and samples. Therefore, Equation (7) provides the form of the fitting function to determine the quantities  $\sigma_f$ ,  $\sigma_0$  and  $m$ , which may be used to describe the fracture behaviors of the sample dies. The data fitting procedure is described in Reference [6].

As long as the three Weibull parameters are determined by curve-fitting the 4-point bend strength data, these three parameters together with Equations (1) and (2), can be used to calculate the die cracking rate in FC-PBGA with similar dies under the same dicing condition.

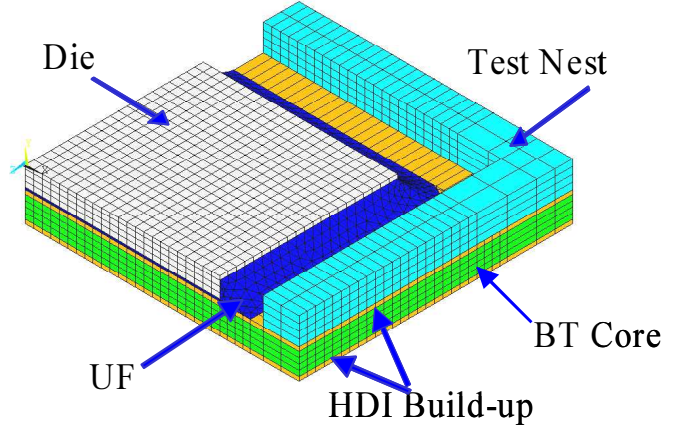


Fig. 2. FEM mesh of an FC-PBGA with test nest. Contact and target elements are used between the nest and the substrate, which are not shown in the figure.

The stress distribution on the surface of the die in an FC-PBGA can be calculated by finite element method (FEM). In the FEM stress calculation, the thermal loading condition is fairly hard to justify. Most of the time, the underfill glass transition temperature, or sometimes the curing temperature is chosen as stress free temperature. Due to some incomplete information about the package such as the unavailable UF and substrate viscoelasticity properties and other issues like UF curing induced strain, the aforementioned stress free temperature criteria are somewhat arbitrary. In order to calculate the accurate die stress in the most critical condition during the product qualification process, we used experiment to assist the FEM calculation. This assistance is realized by measuring the radius of curvature (ROC) of the package at room temperature. FEM is used to calculate a stress-free temperature calibration curve, which is consisted of assumed stress-free temperature as the horizontal axis and corresponding curvature as the vertical axis. The measured ROC is used as a calibration input, together with the FEM calculated calibration curve, to determine the effective stress-free temperature. This determined effective stress temperature can be used for further FEM calculations to obtain the die stress at low temperature during reliability test or in other severe conditions.

## APPLICATION

A practical example is presented here using the methodology described in the previous section. A flip-chip PBGA is electrically tested at  $-40^\circ\text{C}$ . The cold electrical test is conducted on an automatic test handler. This particular handler uses a pushing nest with a hole in the middle. The nest makes contact to the substrate and applies force to the substrate to make the FC-PBGA's C5 balls contacting to the pogo pin array in the socket of the handler. To ensure reliable electric contacts of hundreds of the pogo pins to the C5's, a significant amount of force is applied through the nest.

The FEM mesh considering one quarter of the package and the nest is shown in Figure 2. The whole package can be represented by applying the proper symmetry boundary

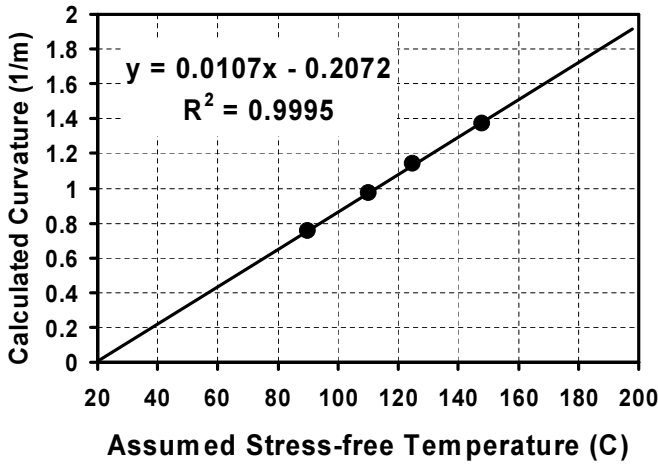


Fig. 3. Stress-free temperature calibration curve. Four assumed stress-free temperatures and their corresponding package curvatures are plotted. A linear regression line is also plotted.

conditions. The top of nest is fixed. The pogo pin effect is modeled by a uniform pressure exerting on the substrate bottom from below since the springs in the pogo pins are soft.

A general purpose FEM software ANSYS [11] is used to model the problem. C4 solder bumps are neglected since their volume is much smaller than the UF and their plasticity and creep make their contribution to die stress further negligible. Previous study has shown that the C5's contribution to die stress also can be neglected due to plasticity and creep [12]. 8-node solid elements are used. The nest and the substrate are modeled as a contact pair. 4-node surface-to-surface deformable contact elements and target elements are used to model the contact behavior. Friction between the nest and the substrate is also considered.

In order to count in the viscoelastic effect of the UF and the substrate in addition to other unknown factors, the stress free temperature calibration curve is calculated first. In this calculation, only the thermal load is applied, and the test nest is not considered. The final temperature is set to be the room temperature (20°C). Several assumed initial or stress-free temperatures are used to calculate the corresponding package curvature at room temperatures. Figure 3 is the results with a linear regression curve.

The package curvature at room temperature is measured by a laser profilometer. The average curvature of the FC-PBGA is 1.081 (1/m) over 30 samples. Using the calibration curve in Figure 3, the effective stress-free temperature can be readily determined and found to be 121°C.

The stress of the FC-PBGA package at -40°C is calculated by FEM. The stress-free temperature 121°C is used as an input for the thermal load. The mechanical contact effect between the test nest and the substrate is also considered in this step. Figure 4 shows the three principal stress components on the surface of the die. The die top is nearly under biaxial stress, which is manifested by the similar distributions of the first

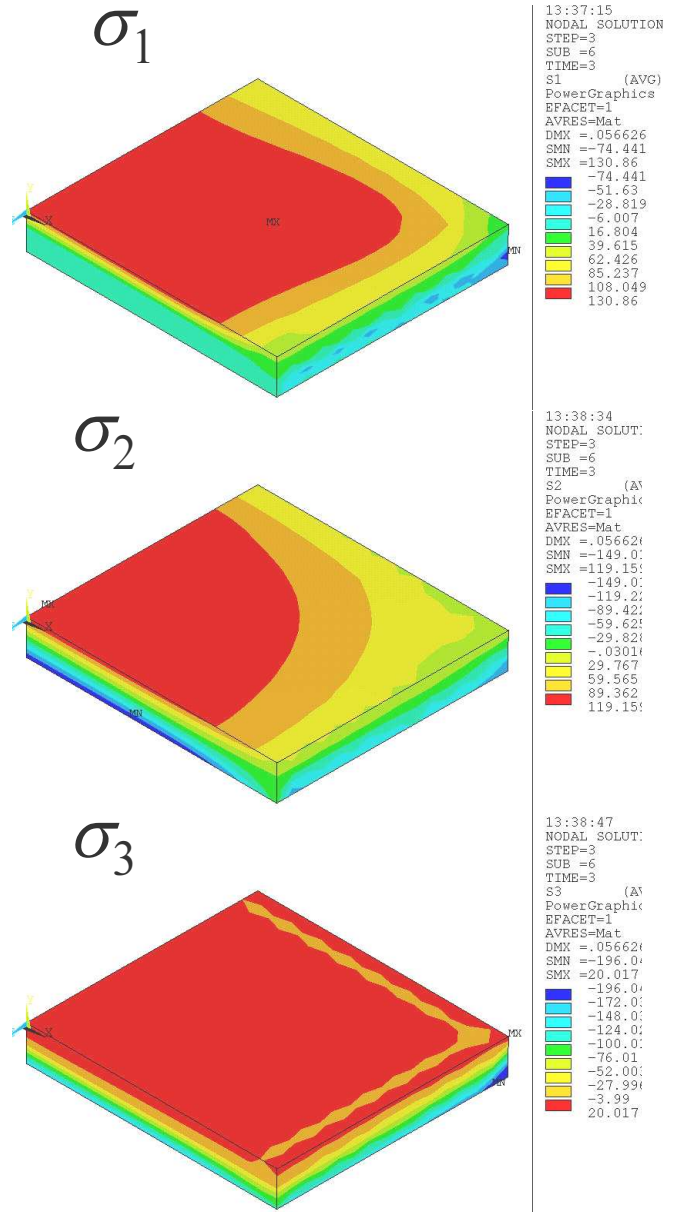


Fig. 4. The three principal stress components on die surface. The stress distribution is calculated at -40°C cold test, which includes the mechanical load caused by test nest and pogo pins. The stress unit is in MPa.

( $\sigma_1$ ) and second ( $\sigma_2$ ) principal stress components. The third ( $\sigma_3$ ) principal stress is near zero on the die top. The slight difference of  $\sigma_1$  and  $\sigma_2$  is due to the rectangular shape of the die.

The contact pressure distribution on the test nest is plotted in Figure 5. It is evident that the pressure between the nest and the substrate is not uniform. The pressure is higher near the inner edge of the nest. This can be understood by considering that the pogo pin array is fully populated underneath the bottom of the substrate and the nest only pushes on the substrate on the peripheral. The force balance requires that the total forces from the pogo pin array and the nest must equal. The force

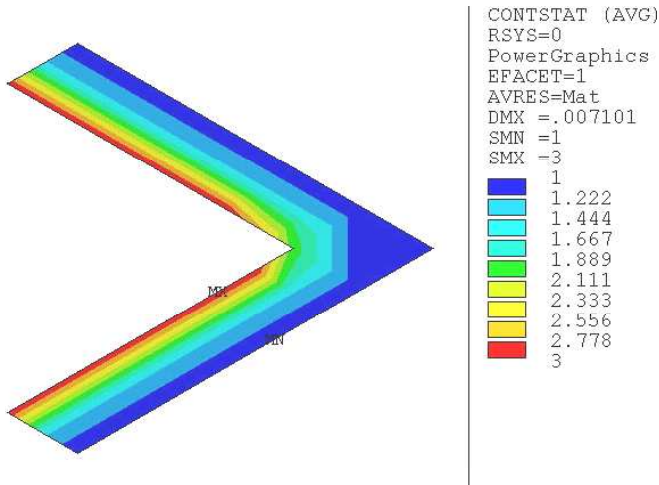


Fig. 5. The contact pressure at the contact surface of the. High pressure near the inside edge indicates the nest flexures substrate during the cold test. The pressure unit is in MPa.

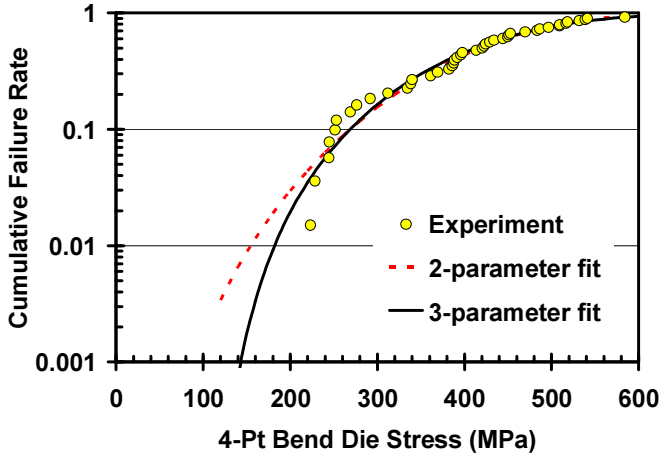


Fig. 6. Die strength tested by 4-point bend in a well-controlled process (Process A). The nominal die stress is the stress at which the die breaks. The dots are experimental data points. The solid line is a curve fitting of the experimental data using Equations (7). The dashed line is a curve fitting using Equation (8)

distribution makes the package experience a flexure moment. In addition to the warpage generated by the thermal mismatch, the nest is pushing on a convex surface. This makes the contact pressure distribution intuitively understandable.

The FEM-predicted die stress can be used to predict the die failure rate. It was found that the die strength is strongly dependent on the process, especially the dicing control. In order to illustrate this point, let's consider two batches of die for the same package. The first batch is produced by a well-controlled process (Process A) and the second is by an uncontrolled process (Process B). 4-point bend die strength data and Weibull fitting curves are given in Figures 6 and 7.

In Figures 6 and 7, the test data are fitted by two schemes.

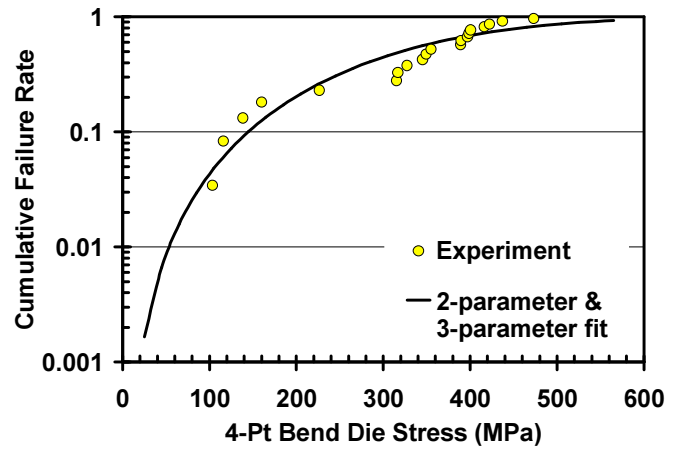


Fig. 7. Die strength tested by 4-point bend in an un-controlled process (Process B). The nominal die stress is the stress at which the die breaks. The dots are experimental data points. The solid line is a curve fitting of the experimental data using Equations (7) and (8). The best fit turns out that  $\sigma_0 = 0$  for the 3-parameter fitting function. Two parameters are sufficient to characterized the die strength of this process.

One is by Equations (7), which consider the multiaxial effect of the stress and three parameters. The other scheme uses the traditional 2-parameter Weibull function Equation (8):

$$P_f = 1 - \exp \left[ - \left( \frac{\sigma_{nom}}{\sigma_f} \right)^m \right] \quad (8)$$

The curve fitting procedure is a least-square best fitting, which is detailed in Reference [6]. In Figure 6, the 2-parameter fitting and 3-parameter fitting are significantly different in the low stress end. The 2-parameter fitting (dashed line) over predicts the failure rate comparing to the 3-parameter fitting (solid line). However, in Figure 7, we started with the 3-parameter fitting, and the least square fitting procedure turned out to have a best fit with a zero cut-off stress,  $\sigma_0 = 0$ . The 2-parameter and 3-parameter fitting procedures produced the same fitting curve, which is shown as the solid line in Figure 7. The fitting parameters are listed in Table 1. It should be noticed that, although Equations (7) and (8) produce the same fitting curve in Figure 7, the fitting parameters are different and they are shown in Table I. The predicted failure probabilities will later be proved to be different for zero cut-off stress as shown in Table II.

Once we have the stress distribution of the die surface and the die strength Weibull distribution parameters  $\sigma_f$ ,  $\sigma_0$  and  $m$ , the stress area integral Equation (2) can be calculated and hence the die failure probability through Equation (1) can be determined. If we take a closer look of Equations (1) and (2), the nominal stress  $\sigma_{nom}$  actually does not contribute to failure probability. It is more convenient to re-write Equations (1) and (2) as the following two equations:

$$P_f = 1 - \exp \left[ - \Gamma \left( \frac{1}{m} + 1 \right)^m \left( \frac{1}{\sigma_f} \right)^m \frac{s(A)}{a} \right] \quad (9)$$



TABLE I

Fitting parameters of the die stress data of Process A and Process B. The stress-area integral Equations (10) and (11) for 3-parameter fitting is also listed in the table.

Process/ Fitting	$m$	$\sigma_f$ (MPa)	$\sigma_0$ (MPa)	$s(A)$ (MPa <sup><math>m</math></sup> ×mm <sup>2</sup> )
A/Eqs. (7, 9,10)	2.827	1086.9	112.9	$2.201 \times 10^4$
A/Eqs. (7, 9, 11) forcing $\sigma_0 = 0$	4.257	996.2	0	$2.122 \times 10^{10}$
A/Eq. (8)	4.257	455.6	0	N/A
B/Eqs. (7, 9, 10)	2.364	1745.2	0	$2.778 \times 10^6$
B/Eq. (8).	2.364	374.4	0	N/A

TABLE II

Die failure rate at  $-40^\circ\text{C}$  cold test for the two processes. Process A is a well-controlled process and Process B is an uncontrolled process.

Process ID	3-para., Eqs.(7, 9, 10)	Eqs.(7, 9, 11), forcing $\sigma_0 = 0$	2-para., Eq. (8)
Process A	$4.29 \times 10^{-7}$	0.24%	0.54%
Process B	4.4%	4.4%	8.0%

and

$$s(A) = \int_A [(\sigma_1 - \sigma_0) H(\sigma_1 - \sigma_0)]^m + [(\sigma_2 - \sigma_0) H(\sigma_2 - \sigma_0)]^m + [(\sigma_3 - \sigma_0) H(\sigma_3 - \sigma_0)]^m dA \quad (10)$$

The actual computation of the stress-area integral Equation (10) was carried out in the postprocessing of the ANSYS FEM result. The numerical integration routine is implemented using ANSYS's "ANSYS Parametric Design Language". In calculation of  $s(A)$ , contributions from all 6 surfaces of the die are considered. The calculated  $s(A)$  is listed in Table I together with the Weibull parameters.

In Table I, for process A, two stress-area integrals are tabulated. One is calculated by Equation (10) the other is calculated the Equation (11), which corresponds to the fitting parameters forcing  $\sigma_0=0$  during the fitting process. This helps us to investigate the effect of stress contribution and multi-axial stress without the 3-parameter effect.

$$s(A) = \int_A [\sigma_1 H(\sigma_1)]^m + [\sigma_2 H(\sigma_2)]^m + [\sigma_3 H(\sigma_3)]^m dA \quad (11)$$

Die failure rates are tabulated in Table II. In the 2-parameter fitting Equation (8), the nominal stress uses the maximum value of the first principal stress on the die top, which is 130.86 MPa in the  $-40^\circ\text{C}$  cold test scenario. For the result of Table II, three points are evident. The first is that the die strength and hence the die failure rate are strongly process-dependent. The second is that the traditional 2-parameter Weibull function Equation (8) (without considering the multi-axial stress and stress distribution) gives much pessimistic predictions. The newly proposed 3-parameter Weibull function considering both multi-axial stress effect and stress distribution produces much realistic perdition. For example, in Process A, the die failure rate is about of  $4.29 \times 10^{-7}$  according to the 3-parameter Weibull fitting. This is better than a "6 $\sigma$ " process [13], which

corresponds to  $3.4 \times 10^{-6}$  failure. For the same process, if the 2-parameter fitting is used, the failure rate is 0.54%, which is not acceptable for volume production. The third important point is that even with multi-axial stress and stress distribution included, if only two parameters are considered, the failure rate is still several orders over-predicted, which is shown in the middle column of Table II for Process A.

Actually, for Process A, no die failure was found in the  $-40^\circ\text{C}$  cold electric test for a sample size of about 2000. This confirms that the process A is a robust process. At the same time, it also validates that the 3-parameter Weibull function considering multi-axial loading and stress distribution is more realistic than the traditional 2-parameter Weibull function without considering multi-axial stress effect and stress distribution.

## CONCLUSIONS

A 3-parameter Weibull distribution cumulative density function form is devised for predicting the die failure rate in FC-PBGAs. This special Weibull function CDF considers both multi-axial stress and stress distribution. The distribution is used to curve-fit the die strength data obtained from 4-point bend test. The newly devised Weibull CDF is applied to FC-PBGA die failure prediction. It provides more aggressive and realistic die failure predictions than traditional Weibull function, which does not consider the multi-axial stress and stress distribution. The application example also shows that dicing control contributes significantly to the die cracking rate for FC-PBGA under harsh testing conditions. A robust FC-PBGA die dicing process, which meets "6 $\sigma$ " quality control requirement, is demonstrated.

## ACKNOWLEDGMENTS

Contributions of Dr. Yifan Guo, Betty Yeung, Zane Johnson on the initial set-up of 4-point bend fixture and helps of Dr. Thomas Koschmieder during the die strength tests are greatly appreciated. Special thanks go to James Guajardo and Trent Uehling for flip-chip assembly support. The author would also

like to thank Dr. Bennett Joiner, Dr. Yuan Yuan and Dave Wontor for their continuous support and useful discussion on this subject.

## REFERENCES

- [1] V. Sarihan and L. Mercado, "Package for an electronic component and a method of making it," US Patent No. US6309908B1, 2001.
- [2] Y. Guo and J.-H. Zhao, "A practical die stress model and its applications in flip-chip packages," *Proceedings of the Seventh Intersociety Conference on Thermal and Thermo-mechanical Phenomena in Electronic Systems (ITHERM 2000)*, pp. 393–399, 2000.
- [3] C. Kittel, *Introduction to solid state physics*, 5th ed. New York: Wiley, 1976.
- [4] G. P. Cherepanov, *Mechanics of brittle fracture*. New York: McGraw-Hill, 1979.
- [5] M. K. Chengalva, "Flip chip die cracking – a simplified approach utilizing experimentation and simulations," *Proceedings of 2002 Inter Society Conference on Thermal Phenomena in Electronic Systems (ITHERM 2002)*, pp. 876–883, 2002.
- [6] J.-H. Zhao, "A three-parameter weibull-like fitting function for flip-chip die strength data," *Microelectronics Reliability*, vol. 44, pp. 459–470, 2004.
- [7] W. Weibull, "A statistical distribution function of wide applicability," *Journal of Applied Mechanics*, vol. 18, pp. 293–297, 1951.
- [8] P. Stanley, H. Fessler, and A. D. Sivill, "An engineer's approach to the prediction of failure probability of brittle components," *Proceedings of British Ceramic Society*, vol. 22, pp. 453–487, 1973.
- [9] J. M. Gere and S. P. Timoshenko, *Mechanics of Materials*, 3rd ed. Boston: PWS-KENT Publishing Company, 1990.
- [10] B. Gross, "Least squares best fit method for the three parameter weibull distribution: Analysis of tensile and bend specimens with volume or surface flaw failure", NASA Technical Memorandum, Tech. Rep. NASA TM-4721, 1996.
- [11] *ANSYS 6.1 User's Manual*, <http://www.ansys.com>
- [12] J.-H. Zhao, Motorola Tech. Rep., 2001.
- [13] Motorola's "Six Sigma" methodology is online at <http://mu.motorola.com/sixsigma.shtml>.